

Development of a large-area ^{3}He tube array neutron detector with frequency reduction capability

Yan-Feng Wang(王艳凤), Li-Xin Zeng(曾莉欣), Liang Xiao(肖亮), Sheng Guo(郭胜), Jing-Jing Ma(马静静), Zhen-Hong Tan(谭振宏), Wu Xie(谢武), Wen-Hai Ji(季文海), Ping Miao(缪平), Hai-Yun Teng(滕海云), Pei-Xun Shen(沈培迅), Qing-Lei Xiu(修青磊), Xing-Feng Jiang(蒋兴奋), Hong Xu(许虹), Xiao-Juan Zhou(周晓娟), Meng-Qi Jiang(蒋孟奇), Lin Zhu(朱林), Lei Hu(胡磊), Jia-Jie Li(李嘉杰), Yong-Xiang Qiu(邱勇翔), Jian Zhuang(庄建), Yu-Bin Zhao(赵豫斌), Yuan-Bo Chen(陈元柏), Jian-Rong Zhou(周健荣), and Zhi-Jia Sun(孙志嘉)

Citation: Chin. Phys. B, 2025, 34 (**11**): 116102. DOI: 10.1088/1674-1056/adfefd
http://cpb.iphy.ac.cn; http://iopscience.iop.org/cpb

What follows is a list of articles you may be interested in

A large-area scintillation neutron detector based on WLSF and SiPM readout

Xiao-Hu Wang(王小胡), Yang-Tu Lu(卢扬图), Bin Tang(唐彬), Xiu-Ku Wang(王修库), Shao-Jia Chen(陈少佳), Ze-Ren Li(李泽仁), and Zhi-Jia Sun(孙志嘉)

Chin. Phys. B, 2025, 34 (**6**): 066106. DOI: 10.1088/1674-1056/adcb1c

Performance optimization of the neutron-sensitive image intensifier used in neutron imaging

Jinhao Tan(谭金昊), Yushou Song(宋玉收), Jianrong Zhou(周健荣), Wenqin Yang(杨文钦), Xingfen Jiang(蒋兴奋), Jie Liu(刘杰), Chaoyue Zhang(张超月), Xiaojuan Zhou(周晓娟), Yuanguang Xia(夏远光), Shulin Liu(刘术林), Baojun Yan(闫保军), Hui Liu(刘辉), Songlin Wang(王松林), Yubin Zhao(赵豫斌), Jian Zhuang(庄建), Zhijia Sun(孙志嘉), and Yuanbo Chen(陈元柏)

Chin. Phys. B, 2024, 33 (**8**): 086102. DOI: 10.1088/1674-1056/ad47ad

Three-dimensional crystal defect imaging by STEM depth sectioning

Ryo Ishikawa, Naoya Shibata, and Yuichi Ikuhara

Chin. Phys. B, 2024, 33 (**8**): 086101. DOI: 10.1088/1674-1056/ad4ff9

Electronic and thermal properties of Ag-doped single crystal zinc oxide via laser-induced technique

Huan Xing(邢欢), Hui-Qiong Wang(王惠琼), Tinglu Song(宋廷鲁), Chunli Li(李纯莉), Yang Dai(戴扬), Gengming Fu(傅耿明), Junyong Kang(康俊勇), and Jin-Cheng Zheng(郑金成)

Chin. Phys. B, 2023, 32 (**6**): 066107. DOI: 10.1088/1674-1056/acae74

First neutron Bragg-edge imaging experimental results at CSNS

Jie Chen(陈洁), Zhijian Tan(谭志坚), Weiqiang Liu(刘玮强), Sihao Deng(邓司浩), Shengxiang Wang(王声翔), Liyi Wang(王立毅), Haibiao Zheng(郑海彪), Huaile Lu(卢怀乐), Feiran Shen(沈斐然), Jiazheng Hao(郝嘉政), Xiaojuan Zhou(周晓娟), Jianrong Zhou(周健荣), Zhijia Sun(孙志嘉), Lunhua He(何伦华), and Tianjiao Liang(梁天骄)

Chin. Phys. B, 2021, 30 (**9**): 096106. DOI: 10.1088/1674-1056/ac0da7

INSTRUMENTATION AND MEASUREMENT

Development of a large-area ^{3}He tube array neutron detector with frequency reduction capability

Yan-Feng Wang(王艳凤)[1,2], Li-Xin Zeng(曾莉欣)[1,2], Liang Xiao(肖亮)[1,2], Sheng Guo(郭胜)[3], Jing-Jing Ma(马静静)[1,2], Zhen-Hong Tan(谭振宏)[1,2], Wu Xie(谢武)[1,2], Wen-Hai Ji(季文海)[1,2], Ping Miao(缪平)[1,2], Hai-Yun Teng(滕海云)[1,2], Pei-Xun Shen(沈培迅)[1,2], Qing-Lei Xiu(修青磊)[1,2], Xing-Fen Jiang(蒋兴奋)[1,2], Hong Xu(许虹)[1,2], Xiao-Juan Zhou(周晓娟)[1,2], Meng-Qi Jiang(蒋孟奇)[1,2], Lin Zhu(朱林)[1,2], Lei Hu(胡磊)[1,2], Jia-Jie Li(李嘉杰)[1,2], Yong-Xiang Qiu(邱勇翔)[1,2], Jian Zhuang(庄建)[1,2], Yu-Bin Zhao(赵豫斌)[1,2], Yuan-Bo Chen(陈元柏)[1,2], Jian-Rong Zhou(周健荣)[1,2,†], and Zhi-Jia Sun(孙志嘉)[1,2,‡]

[1] *Spallation Neutron Source Science Center, Dongguan* 523803, *China*
[2] *Institute of High Energy Physics, Chinese Academy of Sciences, Beijing* 100049, *China*
[3] *School of Physical and Engineering, Tongji University, Shanghai* 200092, *China*

(Received 25 June 2025; revised manuscript received 13 August 2025; accepted manuscript online 26 August 2025)

The time-of-flight high-resolution neutron diffractometer (TREND) at the China Spallation Neutron Source (CSNS) has been successfully equipped with a large-area ^{3}He tube array neutron detector, designed to achieve exceptional resolution and uniformity. The detector system, comprising 14 banks and 134 modules with 1376 ^{3}He tubes, is optimized for high-angle and medium-to-low-angle measurements. Advanced dual-end readout electronics ensure precise charge and time-of-flight measurements, while rigorous performance testing confirmed the system's spatial resolution and uniformity. *In-situ* testing using polyethylene samples validated the detector's operational stability, with counting rate deviations within 3.7%. The system also demonstrated excellent two-dimensional imaging capabilities and adaptability to various neutron wavelength ranges through harmonic division techniques. These results highlight the TREND detector system as a robust and versatile tool for high-resolution neutron diffraction studies.

Keywords: ^{3}He tube detector, time-of-flight, spatial resolution, neutron diffractometer

PACS: 61.05.F–, 28.20.Cz, 29.40.Gx, 28.20.Pr

DOI: 10.1088/1674-1056/adfefd **CSTR:** 32038.14.CPB.adfefd

1. Introduction

The China Spallation Neutron Source (CSNS) is set to host more than twenty neutron instruments. To meet the full range of experimental demands for detection efficiency, spatial resolution, temporal resolution, and field of view, each instrument has been equipped with a customized, diversified suite of neutron detectors: gas-ionization devices centered on position-sensitive ^{3}He tubes, scintillation assemblies built around ^{6}LiF/ZnS(Ag) scintillators coupled to wavelength-shifting fibers and SiPM, and imaging-dedicated detectors.[1–3]

This flexible architecture enables precise measurements spanning millimeter to sub-millimeter spatial resolution, microsecond to nanosecond temporal resolution, and energy resolutions from meV to keV.

The time-of-flight high-resolution neutron diffractometer (TREND), a newly constructed instrument at the CSNS,[4–6] represents a significant advancement in neutron diffraction technology. This state-of-the-art spectrometer combines exceptional resolution with remarkable flexibility in adjusting resolution and brightness parameters.

At the heart of TREND lies a sophisticated large-area ^{3}He tube array neutron detector, strategically positioned within the spectrometer's scattering chamber. The detector system is distributed around the sample scattering chamber (as illustrated in Fig. 1), situated approximately 78 m from the beamline. To optimize performance and meet specific experimental requirements, the neutron detector is systematically organized into 14 distinct banks, comprising 134 detector modules that incorporate 1376 specialized ^{3}He tubes.

The detector configuration is strategically divided based on angular coverage.

High-angle detection (banks 01–06): (1) Utilizes vertically arranged modules with 8 mm diameter ^{3}He tubes (600 mm length). (2) Operates at a filling pressure of 20 atm. (3) Features 38 detector modules containing 608 ^{3}He tubes. (4) Banks 01, 03, 04, and 06 each house 6 modules, while banks 02 and 05 contain 7 modules. Each module integrates 16 ^{3}He tubes with 2 electronic sets.

Medium to low-angle detection (banks 07–14): (1) Em-

†Corresponding author. E-mail: zhoujr@ihep.ac.cn
‡Corresponding author. E-mail: sunzj@ihep.ac.cn

© 2025 Chinese Physical Society and IOP Publishing Ltd. All rights, including for text and data mining, AI training, and similar technologies, are reserved.

ploys horizontally arranged modules with 12.7 mm diameter ^{3}He tubes (600 mm length). (2) Operates at a reduced filling pressure of 15 atm. (3) Comprises 96 detector modules containing 768 ^{3}He tubes. (4) Each bank contains 12 detector modules. Each module consists of 8 tubes with 1 electronic set.

The detailed specifications of the ^{3}He tubes in the TREND detector system are comprehensively presented in Table 1. This optimized detector configuration ensures superior performance across a wide range of scattering angles, making TREND a versatile and powerful tool for advanced neutron diffraction studies.

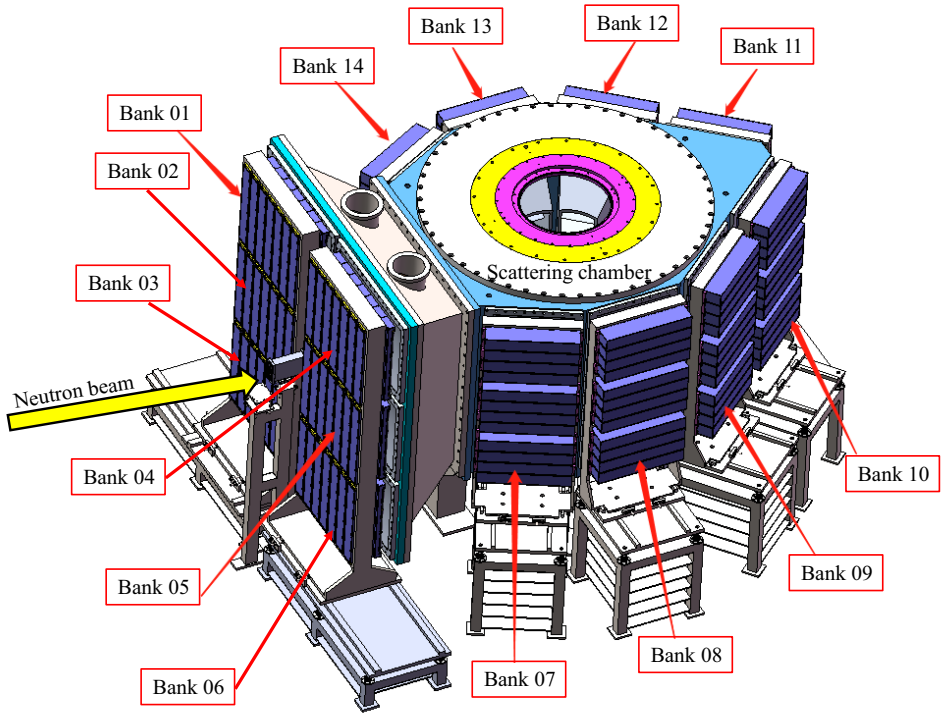


Fig. 1. Layout of the neutron detector in the TREND.

Table 1. Parameters of the ^{3}He tubes in the TREND.

Parameters	Banks 01–06	Banks 07, 14	Banks 08, 13	Banks 09, 12	Banks 10, 11
Diameter	8 mm	1/2 inch	1/2 inch	1/2 inch	1/2 inch
Length	600 mm	600 mm	600 mm	600 mm	600 mm
Position resolution	8 mm	8 mm	8 mm	8 mm	8 mm
Arrangement	Vertical	Horizontal	Horizontal	Horizontal	Horizontal
^{3}He pressure	20 atm	15 atm	15 atm	15 atm	15 atm
Quantity	608		768		

2. Electronics of ^{3}He detector and DAQ

The readout electronics of TREND's main detector system are composed of two key components: front-end electronics and digital electronics. Each detector module is equipped with two front-end electronics units and one digital electronics unit, forming an integrated detector unit. The system employs a sophisticated dual-end readout scheme, where each front-end electronics unit processes signals from eight ^{3}He tubes through eight dedicated input channels. These units perform essential signal preprocessing to meet the stringent requirements of the digital electronics.

The digital electronics unit,[7] located at the backend, features sixteen input channels that receive the preprocessed signals from the front-end electronics. This unit is responsible for critical functions including signal digitization, time-of-flight (TOF) calculation, and charge measurement of incident neutrons. The processed data is then efficiently packaged and transmitted to the data acquisition (DAQ) system for further analysis.

The performance specifications of the ^{3}He tube readout electronics, as detailed in Table 2, are designed to exceed the overall detector performance requirements. Key specifications include: charge measurement range: 10 to 800 fC, charge resolution: < 15 fC, charge integral nonlinearity: $< 1\%$ (within 10–800 fC range), time resolution: < 1 μs, maximum counting rate per channel: ≥ 100 kHz.

The detector system's 1376 tubes, combined with the dual-end readout scheme, necessitate a total of 2752 readout channels. To ensure long-term operational reliability, the system incorporates comprehensive monitoring capabilities, in-

cluding board-level temperature, humidity, voltage, and current monitoring.

Table 2. Design specifications of the readout electronics.

Specification	Value
Number of channels	2752
Charge measurement dynamic range	10–800 fC
Charge resolution	< 15 fC
Charge integral nonlinearity	$< 1\%$ @ 10–800 fC
Time measurement range	40 ms
Time resolution	< 1 μs
Maximum counting rate per channel	> 100 kHz

2.1. Front-end electronics design

The 8-channel front-end electronics design for the ^{3}He tube detector, illustrated in Fig. 2, employs a robust signal processing architecture. Signals are extracted from both ends of the detector and transmitted through a 10 nF high-voltage blocking capacitor to a charge-sensitive preamplifier.

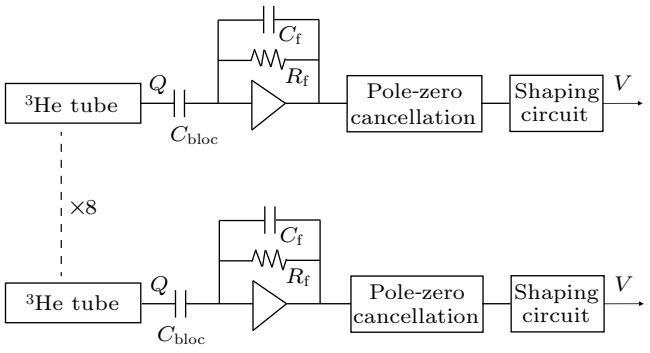


Fig. 2. Front-end electronics block diagram.

The preamplifier utilizes the OPA657 operational amplifier, configured with a feedback capacitance (C_f) of 1 pF and feedback resistance (R_f) of 10 MΩ, achieving a gain of 1 mV/fC and an $R_f \times C_f$ time constant of 10 μs. The shaping circuit time constant is optimized based on signal counting rates and permissible signal pile-up probabilities.

2.2. Data acquisition system architecture

The TREND DAQ system's software architecture, shown in Fig. 3, features a sophisticated interface structure that facilitates seamless interaction between various system components. The readout system software[8] manages critical functions including: detector and electronics system control, data acquisition and processing, PV state machine communication with the control system, alarm information submission, event processing (X, Y, TOF) and Kafka system integration.

The standardized data format includes essential parameters: pulse information (PulseID), pixel information (PixelID), time-of-flight information (TOF). The system's external interfaces encompass: neutron detector system (NDS) for front-end data acquisition, electronics and analysis system (EAS), offline data preprocessing, detector data analysis, physical analysis group (DAG) interface specifications, experiment control (EC) PV interfaces.

This comprehensive architecture ensures efficient data flow and system integration, supporting advanced neutron detection and analysis capabilities.

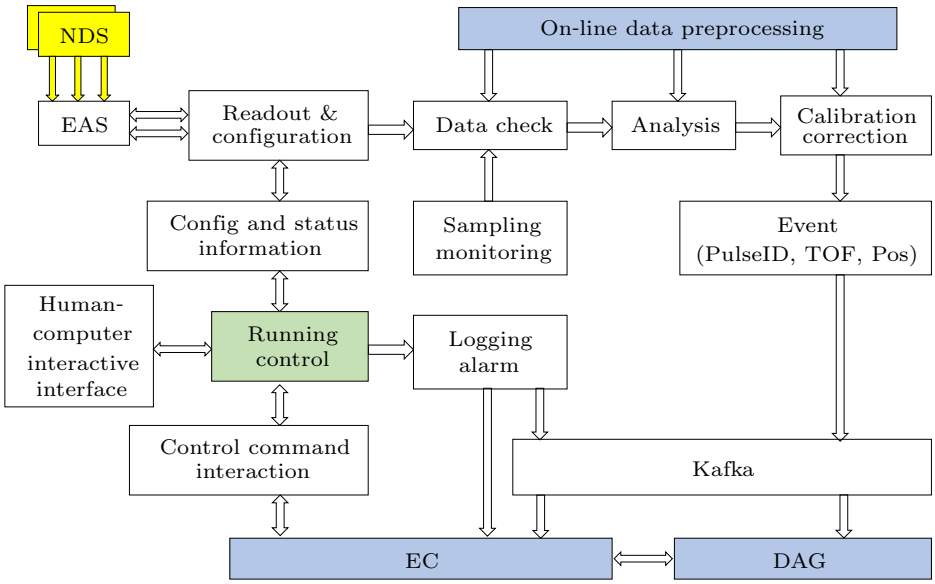


Fig. 3. Data readout system software architecture.

3. Performance testing of neutron detector

Each module comprises 16 ^{3}He tubes, with 8 tubes paired with one electronic system unit, which includes two front-end boards and one digital board. To protect the electronic components from scattered neutron radiation, the electronic system is positioned behind the ^{3}He tube array, shielded by a 10 mm boron-loaded ceramic plate.

A dedicated testing platform has been developed in the

laboratory to evaluate the performance of the ^{3}He tube array detector. This platform supports simultaneous testing of both single-module and multi-module systems and is equipped with essential components such as high-voltage and low-voltage power supplies, T0 devices, and network equipment, enabling the concurrent testing of up to 80 detector modules.

Because ^{3}He-tube measurements are sensitive to temperature and humidity, all detector tests were conducted in the CSNS target station hall under a strictly controlled environment (25 ± 2 °C, 55%–60% relative humidity).

3.1. Module assembly and preparation

Prior to module assembly, all components are meticulously cleaned with alcohol. A 1 cm thick boron carbide ceramic plate is installed on the module's incident surface to block neutrons and shield the electronic system, shown in Fig. 4(a). To ensure signal clarity and prevent interference, each high-voltage cable is fitted with an aluminum braided ground wire, shown in Fig. 4(b). At the interface of each ^{3}He tube, a 1 mm thick silicone layer is applied for insulation to minimize high-voltage sparking, shown in Fig. 4(c). Additionally, the resistance of each ^{3}He tube is repeatedly tested to prevent operational failures due to broken wires, shown in Fig. 4(d). Figure 4 illustrates the critical steps in the installation process of the ^{3}He tube detector.



Fig. 4. Assembly of detector modules.

3.2. High-voltage sparking and noise management

High-voltage sparking can result from various factors, including environmental temperature, humidity, and burrs on high-voltage welding joints. During testing, it is essential to analyze data and phenomena to identify specific causes and implement appropriate solutions. In the background noise testing of the 1376 ^{3}He tubes, some required deburring of high-voltage connectors, while others needed extended aging or operation in low-humidity environments to return to normal noise levels. For example, the high-angle module B1LM04, tested in August and October, showed that after extended aging and controlling environmental humidity below 60%, the noise level of the tube returned to normal.

3.3. Performance testing and calibration

Before installation into the TREND scattering chamber, each module and tube undergoes rigorous performance testing and position calibration on the test beamline to ensure compliance with spectrometer requirements. Only modules and tubes meeting the criteria are installed. Figure 5(a) shows the simultaneous testing of detector modules on the testing beamline. A boron carbide-aluminum substrate serves as the neutron shielding material, with a 3 mm thick boron carbide-aluminum substrate slit array used at the front end of the ^{3}He tubes as the neutron incident surface. In the optical path, 10 mm thick polyethylene is employed to scatter neutrons uniformly onto the slit array of each detector module, facilitating performance testing and position calibration of each tube, shown in Fig. 5(b).

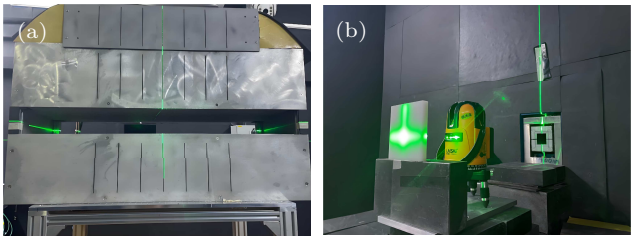


Fig. 5. Neutron detector testing site.

3.3.1. Position reconstruction and spatial resolution

The position reconstruction of the detector is performed using the charge gravity method, [9] as described by the following equation:

$$x = \frac{L(Q_a - Q_b)}{2(Q_a + Q_b)}, \tag{1}$$

$$x' = b + k \times x. \tag{2}$$

Here, x is the position reconstructed by the charge centroid method, L is the length of the tube, Q_a and Q_b are the charges collected at the two ends of the ^{3}He tube. x' represents the true position of the thermal neutron, with a linear relationship between x' and x.

During the spatial resolution test, a ^{3}He tube with an effective length of 600 mm uses a slit array with 7 slits, each 2 mm wide and spaced 80 mm apart. Figure 6(a) shows the linear calibration of the scaling coefficients b and k between x' and x for the position resolution of 8 ^{3}He tubes. Figure 6(b) displays the neutron distribution of a single ^{3}He tube after calibration.

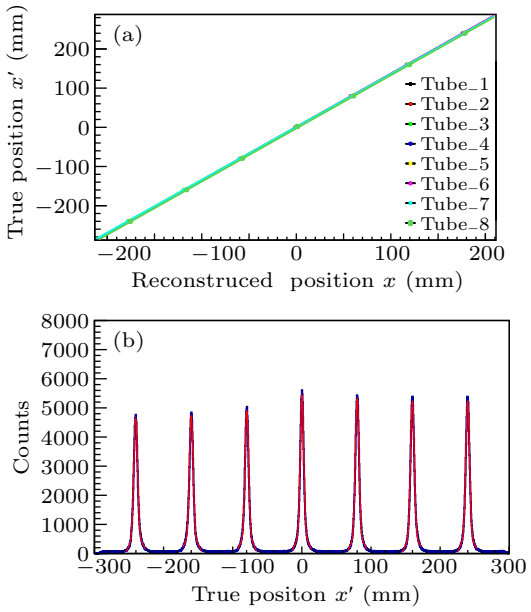


Fig. 6. Position linear calibration and position resolution tests.

The position resolution at each slit is determined by Gaussian fitting. Before calibration, the resolution is within 6 mm, shown in Fig. 7(a). After calibration, it remains within 8 mm, shown in Fig. 7(b). The position resolution in the middle of the ^{3}He tube is superior to that at the edges.[10,11] All position resolutions meet TREND's requirements.

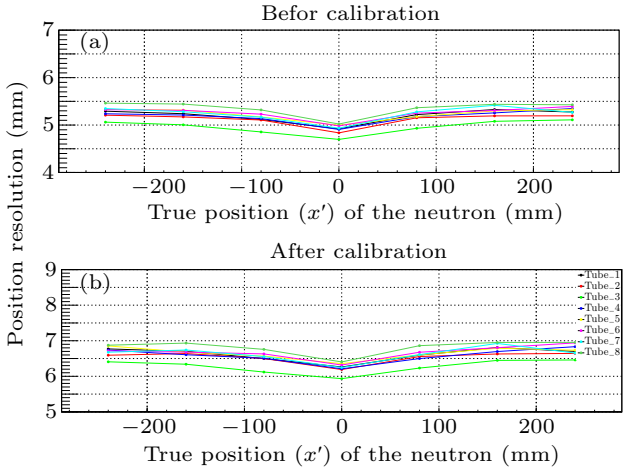


Fig. 7. Position resolution in different regions of the ^{3}He tube.

3.3.2. Imaging capabilities

The TREND large-area ^{3}He tube array neutron detector, utilizing 15 atm or 20 atm of ^{3}He gas, ensures consistent detection efficiency and excellent uniformity (Fig. 8). It also features two-dimensional imaging capabilities. After calibration, the imaging of each slit on different tubes effectively presents the slit position. Each detector module has a set of independent calibration coefficients for each tube, and optimizing these coefficients can further enhance the two-dimensional imaging performance of the neutron detector.

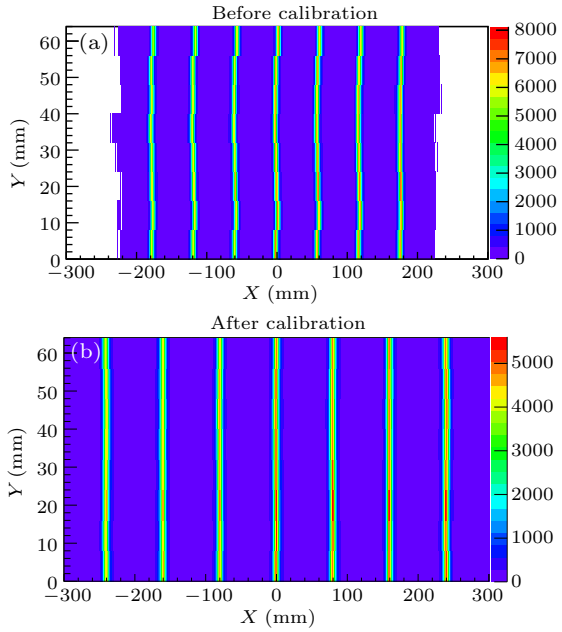


Fig. 8. Slit imaging (a) before calibration and (b) after calibration.

3.4. *In-situ* testing at TREND

Following the installation of all detectors in the TREND scattering chamber, the large-area ^{3}He tube detector system underwent comprehensive testing using a polyethylene sample.

3.4.1. Beam frequency modulation and wavelength range

The neutron beam at the CSNS operates at a high original frequency of 25 Hz. To accommodate TREND's measurement requirements across different neutron wavelength ranges, a chopper system is employed to modulate the high-frequency neutron beam into lower-frequency pulses.

For instance, to achieve a 2nd harmonic division, the chopper allows thermal neutrons from the preceding pulse group to pass while blocking subsequent pulse groups at the next frequency. This principle similarly applies to the 3rd, 4th, and 5th harmonic divisions. Through this frequency reduction mechanism, TREND is capable of conducting measurements within the 0–10 Å wavelength range. Figure 9 illustrates the time-of-flight spectrum of the polyethylene sample under 5th harmonic division conditions.

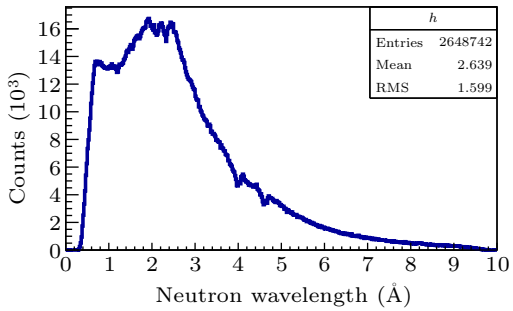


Fig. 9. The time-of-flight spectrum of the polyethylene sample.

3.4.2. Detector system testing and optimization

The large-area ^{3}He tube neutron detector system underwent rigorous testing using polyethylene samples to verify the effective reception of scattered neutron signals by each detector module and individual ^{3}He tube. During the testing process, critical parameters such as high voltage and threshold were carefully adjusted to optimize the uniformity of the detector system.

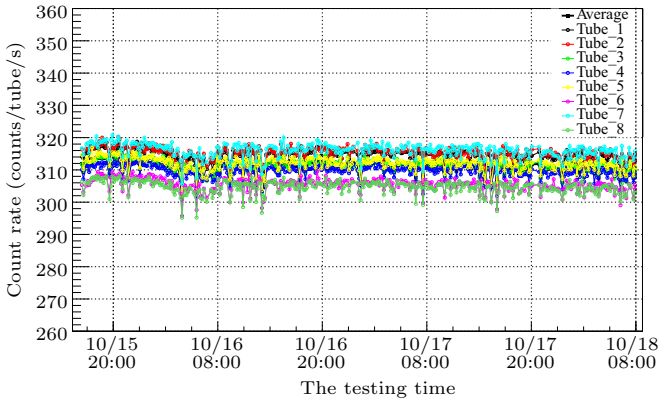


Fig. 10. The counting rate test for detector module B06M08.

The system was tested continuously from 16:20 on October 15, 2024 to 07:20 on October 18, 2024, during which all modules operated without any anomalies. As illustrated in Fig. 10, the counting rate test for detector module revealed consistent performance across its eight ^{3}He tubes, with an average counting rate of 310.974 cps. The maximum deviation in counting rates among the tubes was within 3.7%, a result that also accounts for the inherent inhomogeneity in the scattered neutron distribution from the polyethylene sample. This demonstrates the system's high level of uniformity and reliability under operational conditions.

This *in-situ* testing confirmed the operational stability and uniformity of the ^{3}He tube detector system, ensuring its readiness for high-precision neutron detection and measurement tasks.

4. Conclusion

The large-area ^{3}He tube neutron detector system for the TREND at CSNS has been successfully developed, tested, and validated, demonstrating outstanding performance in neutron detection and measurement. The system's advanced electronics, optimized spatial resolution, and uniformity ensure it meets the stringent requirements of high-resolution neutron diffraction. *In-situ* testing using polyethylene samples confirmed the system's stability, with minimal counting rate deviations and excellent uniformity. Additionally, the detector's two-dimensional imaging capabilities and adaptability to different neutron wavelength ranges through harmonic division further enhance its versatility. These achievements position the TREND detector system as a powerful and reliable tool for advanced neutron diffraction research, enabling groundbreaking studies in related fields.

Acknowledgements

This work was supported by the National Natural Science Foundation of China through the Young Fund Project titled "Research on Polarized Neutron Detector System" (Project Approval No. 12205326).

Additional support was provided by the Guangdong Major Project of Basic and Applied Basic Research (Grant No. 2023B0303000003) and the Guangdong Provincial Key Laboratory of Advanced Particle Detection Technology (Grant No. 2024B1212010005).

References

[1] Wang X H, Lu Y T, Tang B, Wang X K, Chen S J, Li Z R and Sun Z J 2025 *Chin. Phys. B* **34** 066106

[2] Yue X P, Zhu Z F, Tang B, Huang C, Yu Q, Chen S J, Wang X K, Xu H, Zhou S H, Cai X J, Yang H, Wang Z Y, Sun Z J and Liu Y T 2023 *Chin. Phys. B* **32** 090402

[3] Cai X J, Yu Q, Huang C, Tang B, Zhou S H, Wang X H, Yue X P and Sun Z J 2023 *Chin. Phys. B* **32** 110701

[4] Wang F W, Liang T J, Yin W, Yu Q Z, He L H, Tao J Z, Zhu T, Jia X J and Zhang S Y 2013 *Sci. China Phys. Mech. Astron.* **56** 2410

[5] Chen H S and Wang X L 2016 *Nat. Mater.* **15** 689

[6] Chen H S, Chen Y B, Fu S N, *et al.* 2025 *Nucl. Instrum. Methods Phys. Res. A* **1078** 170431

[7] Wu X G, Zhao Y B, Luo H, Zhou J R, Xiao L, Huang T C, Zhou X J, Guan B J, Tian X C, Zhu L, Jiang X F and Sun Z J 2021 *Radiat. Detect. Technol. Methods* **5** 200

[8] Zhu L, Zhou T R, Xia Y G, *et al.* 2023 *Nucl. Sci. Tech.* **34** 1

[9] Zhu L, Zhou J R, Jiang X F, *et al.* 2023 *Radiat. Detect. Technol. Methods* **7** 100

[10] Bönisch S P, Namaschk B and Wulf F 2007 *Nucl. Instrum. Methods Phys. Res. A* **570** 133

[11] Ravazzani A, Para A F, Jaime R, Looman M, Ferrer M M, Peerani P and Schillebeeckx P 2006 *Radiat. Meas.* **41** 582